Final Report on Proposal for

TWENTY-TWO MICRON LUNAR SCANNING PROGRAM

National Aeronautics and Space Administration
NGR 03-002-116

F.J. Low
University of Arizona

Infrared scanning techniques at 22 microns were developed and applied to mapping of the Lunar surface, in order to determine nighttime Lunar temperatures. This work was carried out utilizing the 28-inch telescope at the Catalina Observatory. The data were recorded in the form of raster scans which could readily be digitized and further analyzed. Analyses of the data were carried out by Mr. Wendell Mendell at the Manned Spacecraft Center. The results of this analysis are given in a Master's thesis submitted to Rice University in Houston, Texas by Mr. Mendell. In addition, Mendell and Low* have published some of this material in the attached reprint. As a result of this program, it became clear that the infrared scanning technique is a powerful tool for studying the thermo-physical properties of the Lunar surface. The infrared scanning radiometer experiment on Apollo 17 was a direct outgrowth of this work.

*"Low Resolution Differential Drift Scans of the Moon at 22 Microns", F.J. Low and W. Mendell, J.G.R. 75, No. 17, 3319-3324, 1970.

A70-33646

Low-Resolution Differential Drift Scans of the Moon at 22 Microns

W. W. MENDELL

Manned Spacecraft Center, NASA, Houston, Texas 77058
Rice University, Houston, Texas 77001

F. J. LOW

Lunar and Planetary Laboratory, Tucson, Arizona 85702
Rice University, Houston, Texas 77001

Differential drift scans were made across the 3-day-old moon at a wavelength of 22 μ with a beamwidth of 2.4 arc min. Measured cold-limb brightness temperatures ranged from 102°K in the equatorial region to 84°K in the southern polar regions. Certain scans were processed to reveal the temperature distribution from the cold limb to the sunrise terminator. The portion of the lunar 'cooling curve' that was obtained by this method agrees well with the portion measured by previous investigators who made infrared scans from the sunset terminator into unilluminated regions.

INTRODUCTION

Wesselink [1948] solved the lunar-surface thermal problem using the one-dimensional heat equation with the assumption that the thermal conductivity k, the bulk density ρ, and the specific heat c are each constant. The solution contains the single thermal parameter $\gamma = (k\rho c)^{-1/2}$. A choice of γ for the moon, based on infrared data taken during a lunation, is strongly dependent on lunar nighttime measurements [*Krotikov and Shchuko*, 1963]. Although recent work on thermal models involving radiative transport of heat [e.g., *Winter and Saari*, 1968] demonstrates the inadequacy of the homogenous model, the parameter γ is still useful in describing a lunar nighttime cooling curve in which the very low temperature diminishes the role played by radiation between soil particles.

To obtain a cooling curve, investigators have made scans across the sunset terminator into the unilluminated portion of the moon [*Murray and Wildey*, 1964; *Shorthill and Saari*, 1965; *Wildey et al.*, 1967]. An extrapolation of some of some of these data [*Saari*, 1964] suggests an equatorial antisolar point temperature of 104°K. *Low* [1965] measured a mean temperature of 90°K for the cold limb just prior to new moon.

INSTRUMENT DISCUSSION

Differential drift scans across the 3-day-old moon were made on December 22, 1968, from the Catalina Mountains outside Tucson, Arizona. The detector, a low-temperature germanium bolometer operated at 2°K [*Low*, 1961], was used at the focus of a 12-inch Cassegrain telescope. An interference filter with a spectral band width of 17 to 25 μ and with an effective wavelength of 22 μ was placed in front of the detector. The telescope was pointed by means of an altazimuth mounting, and location of the beams on the moon was achieved with a boresighted guide telescope. A large throughput of 2.8×10^{-4} cm²-ster was obtained, and the beamwidth was measured to be 2.4 arc min.

Radiation incident on the detector was chopped by rapidly moving the secondary mirror in the Cassegrain optics between two fixed positions. The signals from the two positions were substracted electronically, and the difference was amplified. The fixed positions at either end of the throw of the mirror corresponded to two beams separated by 5.3 arc min. Background noise originating from the atmosphere and the telescope optics is nearly canceled by this technique.

If the two beams are scanned colinearly across the lunar disk, the instrument output is directly proportional to the difference in flux

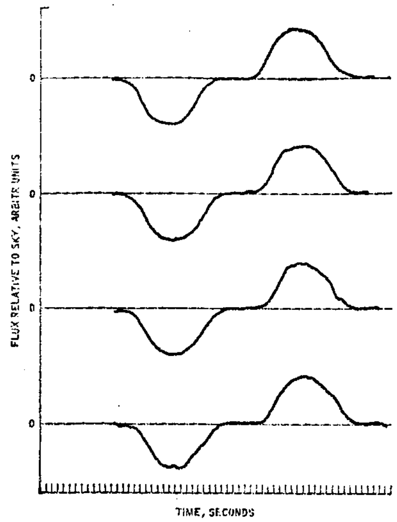

Fig. 1. Four differential drift curves of Venus taken near transit as the planet passed through the two beams.

emitted by the two areas covered by the beams as they progress across the lunar surface. In the reconstruction of the temperature distribution from the signal, misalignment of the scan paths is particularly important if the beam shapes do not have broad, flat, well-defined maxima. A point source passing through two rounded beams at slightly different distances from the centers will cause a false reconstruction. For the case of the drift scans, the beams are spaced in azimuth, while the moon has an altitude component to its motion, so that the beams do not move colinearly across the disk. However, near transit, the altitude component of the motion is small. Therefore, as long as the beams are congruent by translation along the scan and no point sources are encountered by either beam, the trace that would be recorded by a single beam can be reconstructed.

Experimental Results

At the time of observation, the planet Venus was 2° removed from the moon in the sky and was in an excellent position for calibration of the beam pattern. The planetary semidiameter was 8.92 arc sec. Figure 1 shows four drift curves of Venus taken near transit. The beam shape, beamwidth, and spacing of the beams were determined from the normalized drift curves. Since the planetary disk is much smaller than the beam, the curves displayed on Figure 1 represent only a one-dimensional cross section of the pattern. In relating the deflection caused by Venus to the deflection caused by the moon, the beam was assumed to be circularly symmetric.

Figure 2 shows six differential drift scans made across the lunar disk. The variations in amplitude and noise level among the drift scans are partly due to changing the gain of the electronic system. The determination of the limb temperature was made by using the previously measured 22-μ brightness temperature of 248°K for Venus [*Low*, 1966]. The ratio of the lunar-limb deflection to the Venus deflection, corrected for the size of the planetary disk, was taken to be equal to the ratio of the respective fluxes in the spectral bandwidth of the instrument. The lunar-limb temperature was obtained by using a plot of brightness temperature versus flux for an effective wavelength of 22 μ. This technique combines the effect of the atmosphere and the filter. Figure 3 is a diagram of the moon showing the path of these six traces.

As can be seen from the Venus drift curves (Figure 1), the spacing between the beams is larger than the beamwidth. Therefore, the first part of each scan is a direct measure of thermal flux from the lunar limb. Table 1 shows the

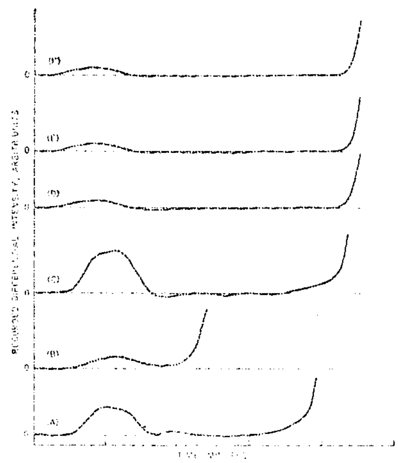

Fig. 2. Six differential drift curves of the lunar disk taken near transit. The deflection caused by the cold west limb is on the left of each scan. Each scan ends on the right where the bright terminator region pegged the recorder. The gain of the amplifier on scans (a) to (c) was 6.3 times that on scans (d) to (f).

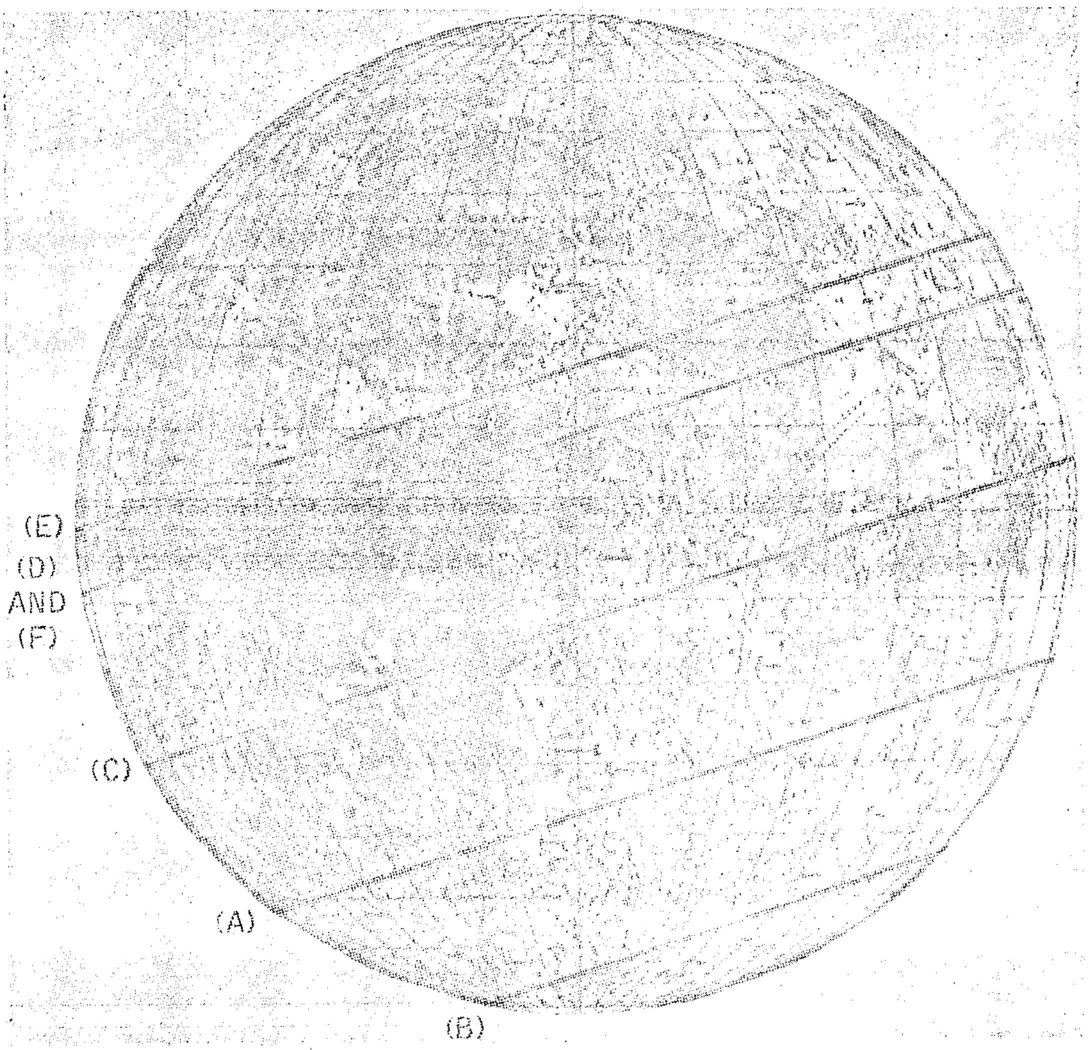

Fig. 3. Paths of the scans shown in Figures 2 and 4.

temperature and location associated with the limb deflection of all scans taken, including those scans taken at large hour angles.

The signal for scan (b), the smallest measured lunar limb deflection, is 33 times the rms sky noise. This ratio increases to 82 for a limb temperature of 95°K. The dominant sources of error lie with the knowledge of the 22-μ temperature of Venus, the effective wavelength of the atmosphere-filter combination, and the correction for the shape of the beam. The total error for the measurement is calculated to be ±3°K at 95°K. Although the temperature error appears small, it represents an uncertainty approaching 20% in the measured flux. In the reconstruction process, there is an accumulation of sky noise and digitizing noise along the scan, but it is small compared to the errors mentioned above.

The uncertainties on the last five deflections [scans (g) to (k)] listed in Table 1 will be somewhat larger. A loss of vacuum in the helium dewar occurred while data were being taken. An analysis of Venus deflections taken after the vacuum had been restored indicates the system may not have reached equilibrium before the later scans were made. An attempt to correct for this condition was made by using Venus

TABLE 1. Calculated Limb Temperatures

Scan	Limb Temp., °K	Location		
		Longitude, deg	Latitude, deg	Description
(a)	94	42 W*	48 S*	North of crater Schiller
(b)	84	10 W*	70 S*	Southern polar regions
(c)	100	47 W*	25 S*	West edge of Mare Humorum
(d)	102	52 W	5 S	Between craters Grimaldi and Flamsteed
(e)	102	53 W	1 N	South of crater Reiner
(f)	102	52 W	5 S	Between craters Grimaldi and Flamsteed
(g)	105 (101)†	53 W	2 S	Between craters Grimaldi and Flamsteed
(h)	105 (102)†	54 W	4 N	South of crater Reiner
(i)	99 (96)†	55 W	24 N	West of crater Aristarchus
(j)	96 (94)†	46 W	37 S	Between crater Schickard and Mare Humorum
(k)	102 (100)†	47 W	25 S	West edge of Mare Humorum

* Estimated.
† Best estimate of temperature following system malfunction.

deflections taken before and after the lunar data. The results are the first temperatures listed for scans (g) to (k). The temperatures in parentheses are those that would be obtained if the earlier Venus deflection were used. The better agreement of the numbers in parentheses with the data of the first few scans indicates that the system may have indeed reached equilibrium and that the problem lay in centering Venus in the beam when the planet had a large altitude component of drift motion.

Discussion of Results

Single-beam scans were reconstructed from the differential drift scans shown in Figure 1 and are displayed in Figure 4. Scan (a) passed across an intense point anomaly which is almost certainly the crater Tycho, the most intense darkside anomaly [*Low and Mendell*, 1968]. The structure on the scan eastward from the anomaly is unrecoverable because of a slight deviation of the sensor alignment from the direction of the drift motion. The reconstruction process generates 'ghost' images of the anomaly along the scan because of incomplete cancellation of the positive deflection by the negative beam.

Scan (b) in Figure 4 passes through the south polar regions. The small step prior to the terminator represents a contribution from the cusp as the beam passes near the cusp. The polar regions might be expected to exhibit the lowest temperatures found on the moon. Therefore the value of 84°K for this scan is somewhat surprising in view of values ≤ 70°K previously reported for this region by *Low* [1965].

The third scan [scan (c)] shows a feature just off the limb. The location corresponds to Mare Humorum, and the enhancement is approximately 1.5°K. This mare is approximately the same size as a resolution element. Otherwise, the trace is essentially featureless, except for an increase in temperature just prior to crossing of the terminator. The steadily increasing nature of the rise indicates that the rise is due to the edge of the sensor encountering the nearby terminator.

Scans (d), (e), and (f) passed over similar areas, including the crater Copernicus. The maximum enhancement caused by the anomaly is approximately 2°K on scan (e). The general trend of the data is a gentle decrease in temperature to about the middle of the disk. The radiance level across Mare Serenitatis appears constant and slightly above that of the midpoint minimum. This general structure is somewhat obscured by reconstruction 'ghosts' of the Copernican anomaly appearing in the data. These three traces were made at an amplifier gain that was a factor of 6.3 less than that of the

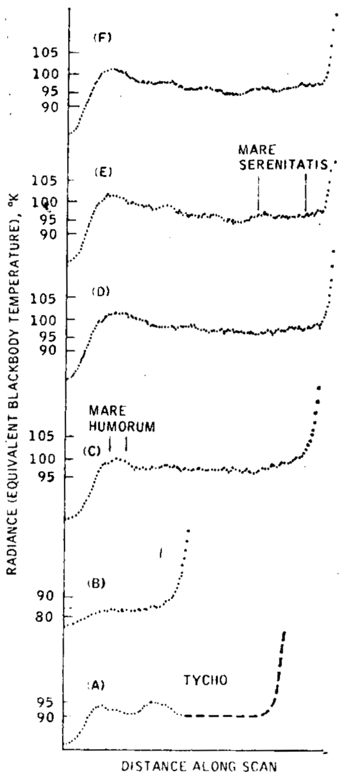

Fig. 4. Reconstructed single-beam scans across the lunar disk.

other three scans. This lower gain reduced the tail of the sensor pattern and made the terminator a much more distinct feature. Thus the preterminator enhancement appears to be real on these scans.

The recorded positions of scans (d) and (f) were essentially the same. The path follows the border of Mare Serenitatis and Mare Tranquillitatis, where it is known from eclipse data that a high concentration of anomalies exists. The collective effect of the hot spots could account for the enhancement prior to the terminator crossing. However, scan (e) is more northerly and crosses Mare Serenitatis proper approximately one-half a beamwidth from the anomaly grouping. The inference that Mare Serenitatis is thermally enhanced can only be regarded as tentative, considering the quality of the data and the suspicious contiguity of the enhancement to the terminator. An enhancement of 2°K for Mare Serenitatis over the temperature in the mountainous highlands to the west would require a difference in the thermal parameter γ of approximately 70 cm^2 deg sec$^{1/2}$ cal^{-1}, an emissivity difference of approximately 0.1, or a combination of the two effects. Possible physical explanations for such an increase in γ might be a relative abundance of meter-sized rocks in the mare or a finer grained soil with an increased contact conductivity (D.F. Winter, personal communication, 1970).

Figure 5 presents the data of scan (d) in conjunction with the data of other investigators who scanned off the sunset terminator. The points attributed to *Wildey et al.* [1967] were taken from curves 11 and 12 in Figure 3 of their paper. These curves were selected because they represent scans taken over much of the same area as scan (d) of Figure 3. The data from *Murray and Wildey* [1964] were shifted five hours toward the terminator, as suggested by *Ingrao et al.* [1966]. The apparent continuity of the curve is good.

The beamwidth of the sensor pattern used in this work is comparable to that of radio telescopes. The data should be useful in in-

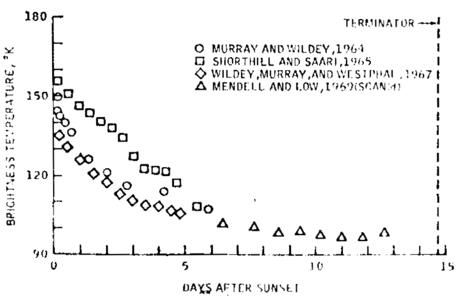

Fig. 5. A comparison of lunar nighttime infrared measurements. The data presented in this figure by *Wildey et al.* [1967] were measured over the same region as covered by scan (d) of this work.

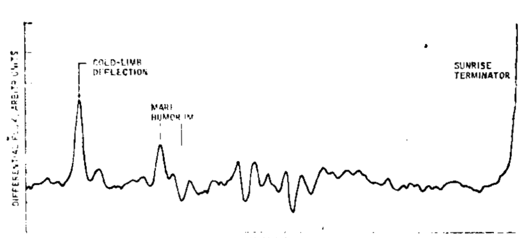

Fig. 6. High-resolution (22 arc sec) scan across the 4-day-old moon of April 1, 1968. The scan path is similar to that of scan (c) on Figure 3.

terpreting results at radio wavelengths since certain theories of lunar radio-emission make explicit use of infrared measurements [*Troitskii*, 1954].

High-resolution scans, such as the one in Figure 6, have been made by using the differential technique. However, the reconstruction process for these traces is extremely sensitive to the stability of the null signal from the two sensors and to the colinearity of the two paths. Currently, high-resolution, quantitative data on postmidnight temperatures are difficult to obtain without a general background temperature map. Further low-resolution scans are planned to provide this needed information.

Acknowledgment. This work was supported by the National Aeronautics and Space Administration under grant NGR 03-002-116

References

Ingrao, H. C., A. T. Young, and J. L. Linsky, A critical analysis of lunar temperature measurements in the infrared, in *The Nature of the Lunar Surface: Proceedings of the 1965 IAU-NASA Symposium*, edited by W. N. Hess, D. H. Menzel, and J. A. O'Keefe, pp. 185–211, Johns Hopkins, Baltimore, 1966.

Krotikov, V. D., and O. B. Shchuko, The heat balance of the lunar surface layer during a lunation, *Soviet Astron.-AJ, 7*, Engl. Transl., 228–232, 1963.

Low, F. J., Low-temperature germanium bolometer, *J. Opt. Soc. Amer., 51*, 1300–1304, 1961.

Low, F. J., Lunar nighttime temperatures measured at 20 microns, *Astrophys. J., 142*, 806–808, 1965.

Low, F. J., Observations of Venus, Jupiter, and Saturn at λ 20μ (abstract), *Astron. J., 71*, 391, 1966.

Low, F. J., and W. W. Mendell, Lunar infrared flux measurements at 22 microns, paper presented at the Planetary Subgroup of the American Astronomical Society, Austin, Texas, Dec. 10, 1968.

Murray, B. C., and R. L. Wildey, Surface temperature variations during the lunar nighttime, *Astrophys. J., 139*, 734–750, 1964.

Saari, J. M., The surface temperature of the antisolar point of the moon, *Icarus, 3*, 161–163, 1964.

Shorthill, R. W., and J. M. Saari, Radiometric and photometric mapping of the moon through a lunation, *Ann. N. Y. Acad. Sci., 123*, 722–739, 1965.

Troitskii, V. S., On the theory of radioemission of the moon, (in Russian), *Astronomicheskii Zhurnal, 31*, 511–528, 1954.

Wesselink, A. J., Heat conductivity and nature of the lunar surface material, *Bull. Astron. Inst. Neth., 10*, 351–363, 1948.

Wildey, R. L., B. C. Murray, and J. A. Westphal, Reconnaissance of infrared emission from the lunar nighttime surface, *J. Geophys. Res., 72*, 3743–3749, 1967.

Winter, D. F., and J. M. Saari, A Particulate Thermophysical Model of the Lunar Soil, *Boeing Sci. Res. Lab. Doc. D1-82-0725*, 1968.

(Received December 8, 1969;
revised February 27, 1970.)